Available online at www.sciencedirect.com
SCIENCE DIRECT®
Journal of Molecular Spectroscopy 219 (2003) 70–80
Journal of MOLECULAR SPECTROSCOPY
www.elsevier.com/locate/jms

Vibrational spectroscopy of *cis*- and *trans*-formic acid in solid argon

Ermelinda M.S. Maçôas,[a,b,*] Jan Lundell,[a] Mika Pettersson,[a] Leonid Khriachtchev,[a] Rui Fausto,[b] and Markku Räsänen[a]

[a] *Laboratory of Physical Chemistry, University of Helsinki, P.O. Box 55 (A.I. Virtasen aukio 1), FIN-00014 Helsinki, Finland*
[b] *Department of Chemistry (CQC), University of Coimbra, P-3004-535 Coimbra, Portugal*

Received 26 September 2002; in revised form 19 December 2002

Abstract

Absorption spectra of *cis* and *trans* conformers of formic acid (HCOOH) isolated in solid argon are analyzed in the mid-infrared (4000–400 cm^{-1}) and near-infrared (7800–4000 cm^{-1}) regions. The HCOOH absorption spectrum reveals matrix-site splitting for the trapped molecule. Narrowband tunable infrared radiation is used to pump a suitable vibrational transition of the *trans* conformer in order to promote site-selectively the conversion to the *cis* conformer and separate the spectral features of each site group. Several anharmonic resonances are identified for both conformers. The results of anharmonic vibrational ab initio calculations (CC-VSCF) for the *trans* and *cis* conformers of formic acid are reported and compared with the experimental spectra.

1. Introduction

Formic acid (HCOOH) is the simplest organic acid exhibiting rotational isomerism with respect to rotation around the single C–O bond. It is a molecule of astrophysical [1] and atmospheric [2] relevance, and has a wide range of industrial applications [3]. Formic acid exists in two stable planar structures, the *cis* and *trans* conformers shown in Fig. 1, with 0° and 180° H–C–O–H dihedral angles, respectively. The *trans* form is the most stable and the predominant one in the gas phase. Gas phase [4–8] and matrix-isolated [9–12] *trans*-formic acid and its isotopomers have been the subject of many spectroscopic studies in the mid-infrared region (mid-IR). Near-infrared (near-IR) spectroscopic data for the gaseous *trans*-HCOOH and its deuterated analogues are also available [13]. Recently, a detailed analysis of the gas-phase vibrational spectrum of *trans*-HCOOH appeared, reporting new overtone and combination data [14]. To the best of our knowledge no near-IR data of matrix-isolated formic acid has been reported yet.

The first reliable identification of *cis*-HCOOH was made in the gas phase by Hocking, where the microwave spectra of isotopically substituted species of *cis*-formic acid were reported [15]. The lack of experimental data concerning this conformer is not surprising considering the relative energy difference of 1365 cm^{-1} between the two conformers [15], leading to a Boltzmann population ratio of $P_{cis} : P_{trans} \approx 10^{-3}$ at 298 K. The thermal decomposition of gaseous formic acid at moderately high temperatures complicates the thermal enhancement of the population of the *cis* form [16]. The assignment of 8 out of the 9 IR-active fundamentals and a few overtones and combination modes of *cis*-formic acid in an argon matrix have been previously reported [17]. In that work, narrowband tunable near-IR radiation was used to convert the *trans* conformer into the *cis* form by pumping the first OH stretching overtone at ca. 6934 cm^{-1}. This excitation is sufficient to surmount the estimated torsional energy barrier (values ranging from $\approx$ 4200 to 4800 cm^{-1} [15,18,19]). It was found that in an argon matrix at 15 K *cis*-HCOOH tunnels back to *trans*-HCOOH with a rate of ca. $2 \times 10^{-3}\ s^{-1}$, limiting the data collection time [17,20].

Splitting of IR absorption bands of matrix-isolated species is a well-known phenomenon usually called matrix-site effect. This splitting is caused by different local environments of the trapped species and potentially provides a way to study local matrix morphology.

* Corresponding author.
E-mail address: emacoas@qui.uc.pt (E.M.S. Maçôas).

0022-2852/03/$ - see front matter © 2003 Elsevier Science (USA). All rights reserved.
doi:10.1016/S0022-2852(03)00018-3

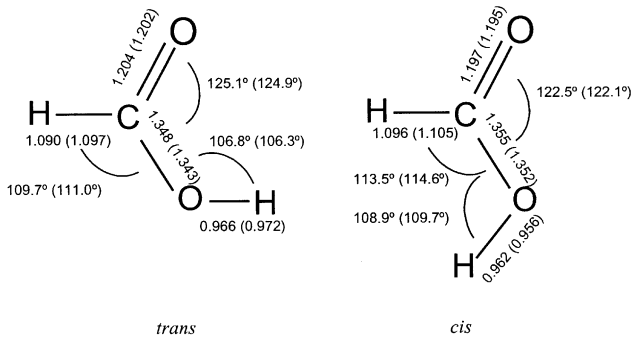

Fig. 1. The two stable conformers of formic acid; *cis*-HCOOH being 1365 cm^{-1} above *trans*-HCOOH [15]. The optimized MP2/6-311++G(2d,2p) geometrical parameters are given together with the experimental values from [30] in parenthesis. Angles are in degrees and bond length in angstroms.

In our studies of HONO and $(FCO)_2$ in rare-gas matrices [21,22], it was found that the interconversion of the isomers with narrowband IR pumping is site-selective and no exchange between site groups was seen. This concept of site-selective optical pumping is also used in the present study.

In this work, the mid-IR absorption spectra of *cis*- and *trans*-HCOOH and DCOOH, as well as the near-IR absorption spectra of *cis*- and *trans*-HCOOH, isolated in different sites in argon matrices at 8 K are analyzed. The near-IR spectra of the matrix-isolated *trans*-DCOOH and *trans*-HCOOD isotopomers are also studied. Additionally, the anharmonic vibrational frequencies for both isomers of HCOOH and DCOOH, derived from correlation-corrected vibrational self-consistent-field calculations (CC-VSCF) [23–26] based on the MP2/6-311++G(2d,2p) computed potential energy surfaces, are reported and the performance of the method is discussed.

2. Experimental

The gaseous samples were prepared by mixing formic acid (KEBO LAB, >99%) or its isotopomers (HCOOD and DCOOD, IT Isotop, 95–98%), degassed by several freeze–pump–thaw cycles, with high purity argon (AGA, 99.9999%), typically in the 1:1000 proportion. The DCOOH species was obtained from DCOOD by exchange with H_2O adsorbed on the inner surface of the sample container and the deposition line. In this way DCOOD:DCOOH ratios of ≈1:5 in the matrix samples were obtained. The gaseous mixtures were deposited onto a cooled CsI substrate kept at 15 K in a closed cycle helium cryostat (APD, DE 202A) and subsequently cooled down to 8 K. The IR absorption spectra (7900–450 cm^{-1}) were measured with a Nicolet SX-60 FTIR spectrometer. A liquid nitrogen cooled MCT detector and a KBr beamsplitter were used to record the mid-IR spectra, with unapodized spectral resolutions from 0.25 to 1.0 cm^{-1}, and a nitrogen cooled InSb detector and a quartz beamsplitter were used for the near-IR spectra, with a spectral resolution of 0.5 cm^{-1}. Typically 128 and 500 interferograms were coadded for the mid-IR and near-IR spectra, respectively.

Tunable (225 nm–4 μm) pulsed IR radiation provided by an optical parametric oscillator (OPO Sunlite, Continuum, with IR and UV extension) was used to induce the *trans* → *cis* isomerization of HCOOH and DCOOH. The pulse duration was ca. 5 ns with a linewidth of ~0.1 cm^{-1}. A Burleigh WA-4500 wavemeter was used to control the OPO radiation wavelength, providing an absolute accuracy better than 1 cm^{-1}. Without pumping, the concentration of the *cis* conformer produced by irradiation of the *trans* form decreases by more than 70% during the time needed to record the spectra. In order to maintain a sufficiently large concentration of the *cis* conformer during long measurements, the IR absorption spectra were recorded under simultaneous IR pumping. For this purpose the pumping beam was nearly parallel to the spectrometer beam and interference filters were used to prevent the scattered laser radiation from reaching the detector. A band pass filter transmitting in the 7900–4000 cm^{-1} region was used to record the spectrum while irradiating the sample in the OH stretching fundamental region of *trans*-HCOOH (3560–3545 cm^{-1}) whereas the 3650–3400, 3300–1000, and 2000–500 cm^{-1} band pass filters were used to record the mid-IR spectra while pumping near-IR active bands. With these filters no interference of the laser radiation on the interferogram was detected.

3. Computational method

The equilibrium structures and harmonic vibrational frequencies of *trans*- and *cis*-HCOOH were calculated using the second-order Møller–Plesset perturbation (MP2) theory with the 6-311++G(2d,2p) basis set. This basis set has been shown to be able to reproduce the experimental structural and vibrational properties of formic acid with an acceptable accuracy [27,28].

The anharmonic vibrational properties of various isotopomers of *trans*- and *cis*-HCOOH were studied by combining the electronic ab initio code GAMESS [29] with the vibrational self-consistent field (VSCF) method and its extension by corrections via second-order perturbation theory [23–26]. This correlation-corrected VSCF (CC-VSCF) method was used to solve the vibrational Schrödinger equation within the normal-mode coordinate system. This procedure involved representing the wavefunction as a product of one-dimensional functions and then solving the resulting equations self-consistently. To make the integrals involved in the CC-VSCF calculation more tractable and to reduce the

number of electronic structure computations required, a pairwise coupling approximation was made to the potential in the normal-mode representation [24]. This approximation provided a grid of points in normal-mode coordinates at which the potential energy was calculated. Each pair of normal modes was pictured with a 16-by-16 potential surface grid, leading to a total of 30 816 points computed at the MP2/6-311++G(2d,2p) level of theory for each isotopomer.

4. Results and discussion

When the deposited samples are kept at 8 K under broadband globar irradiation it is possible to detect very weak bands belonging to the *cis* conformer for HCOOH, DCOOH, and HCOOD. The presence of the less stable conformer in the sample is due to the globar induced isomerization that leads to a photoequilibrium of the *trans* ↔ *cis* interconversion under broadband IR irradiation [22]. The globar induced isomerization processes are suppressed by blocking the radiation above 2000 cm^{-1}. In this case, the presence of the *cis* form was not detected.

The spectra of formic acid in an argon matrix clearly reveal two predominant trapping sites, here labeled as site 1 and site 2. Pumping formic acid site-selectively allows us to distinguish the spectral features of each site. Figs. 2 and 3 present two regions of the mid-IR and near-IR difference spectra demonstrating the results of the site-selective pumping of *trans*-HCOOH. The photo-induced relative population of the *cis* conformers was typically ≈50%.

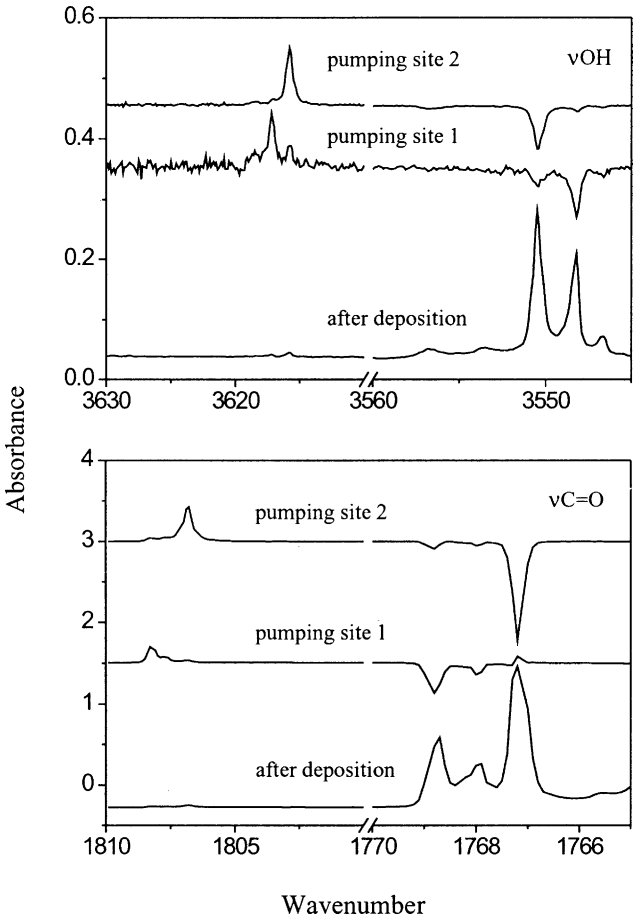

Fig. 2. Fragments of the mid-infrared spectra of HCOOH in solid Ar at 8 K. The as-deposited samples contain the *trans* conformer (lower trace). Pumping of site 1 and site 2 of *trans*-HCOOH gives rise to the *cis* conformer as presented by the difference spectra (middle and upper traces).

5. Mid-IR region

The absorptions of *trans*-formic acid detected at 4183.6 cm^{-1} for site 1 and 4185.2 cm^{-1} for site 2 were used to excite vibrationally HCOOH and promote the site-selective rotamerization, enabling the collection of information about the mid-IR spectrum of both sites (Fig. 2). DCOOH was irradiated at 6933.3 and 6937.4 cm^{-1} in order to promote the photo-isomerization reactions in the corresponding sites 1 and 2. Table 1 shows the observed mid-IR absorptions for the two main sites for both conformers of HCOOH and DCOOH in solid argon together with the anharmonic computational predictions for the vibrational frequencies. The assignments made for both conformers of HCOOH and for *trans*-DCOOH agree with those reported in [10,11,17]. The spectral data for *cis*-DCOOH are reported here for the first time. For some modes (e.g. C=O stretching) the band belonging to the same site appear clearly splitted in several components. This is due to solid state perturbations on the vibrational properties of the guest molecule, which can split the absorption bands by coupling the vibrational transitions with libration motion of the molecule or by the equilibrium between different orientations of the molecule in the same site [21]. The presence of accidentally nearly degenerated sites besides the two main sites can also be responsible for the splitting. Since the vibrational bands for the two sites of the same conformer differ only by a few wavenumbers we will limit the following discussion to the assignment of the vibrational bands originating from the molecules isolated in site 2.

Generally, for a carboxylic group displaying an O=C–O–H dihedral angle of 180° the O–H and C=O stretching vibrations occur at higher wavenumbers (νOH ≈ 3616 and νC=O ≈ 1807 cm^{-1} for *cis*-HCOOH) than in the 0° dihedral angle arrangement (νOH ≈ 3550 and νC=O ≈ 1768 cm^{-1} for *trans*-HCOOH). This is due to the different degree of the [O=C–O–H ↔ O^{-}–C=O^{+}–H] mesomerism in the two conformations, which appears to be slightly less efficient in the higher energy *cis* configuration. This leads to a shortening of

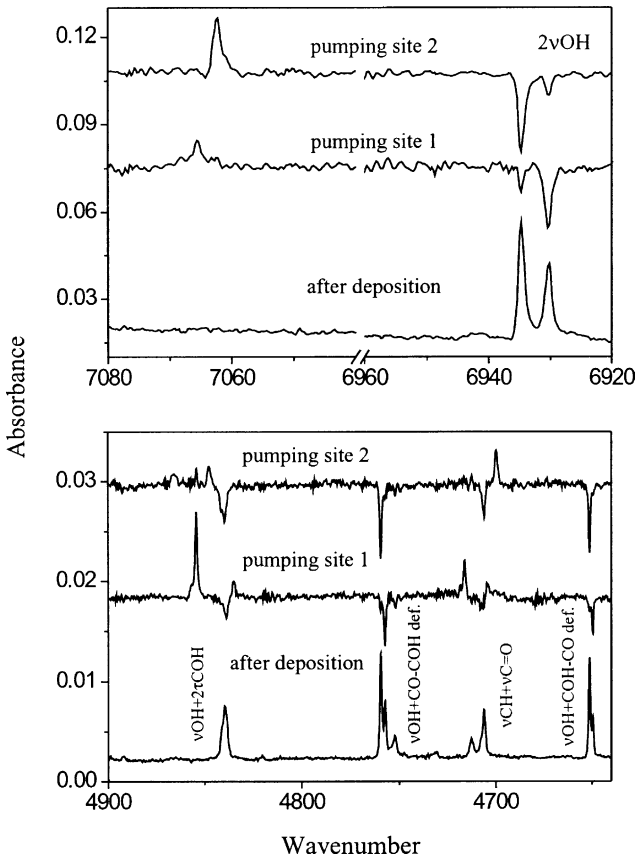

Fig. 3. Fragments of near-infrared spectra of HCOOH in solid Ar at 8 K. The as-deposited samples contain the *trans* conformer (lower trace). Pumping of site 1 and site 2 of *trans*-HCOOH gives rise to the *cis* conformer as presented by the difference spectra (middle and upper traces).

the C=O and O–H bond distances and a lengthening of the C–O bond distance, as well as the decrease of the OCO angle in the *cis* configuration when compared to the *trans* form [15,30,31]. The structural differences arising from the mesomerism do not have a counterpart on the C–O stretching mode (νC–O) because it is generally a very mixed vibration. The observed νOH and νC=O frequencies for both conformers of HCOOH are reproduced by the anharmonic calculations with an accuracy better than 1%.

The C–H rocking fundamental (γCH) of *trans*-HCOOH appears as a weak band at 1381.0 cm^{-1}, in good agreement with the calculations (1388.7 cm^{-1}). For *cis*-HCOOH the weak band observed at 1391.8 cm^{-1} is assigned to the γCH mode in site 2 while the corresponding mode for site 1 could not be detected. The weak band reported in [17] in this region (1396 cm^{-1}) was not observed in the present experiments.

A Fermi resonance doublet was observed for *trans*-HCOOH at 1305.7 and 1215.8 cm^{-1} involving the CO–COH deformation mode (CO–COH def.) and the first overtone of the COH torsion (2τCOH). This resonance is well known and it has been considered to be responsible for the apparent shift of 2τCOH towards higher wavenumbers in *trans*-HCOOH [8,10,11]. Simultaneously, the CO–COH deformation in this conformer is observed at lower wavenumbers when compared with the *cis* form (although it was predicted by the calculations at higher wavenumbers). In the *cis* conformer, the τCOH overtone is 270 cm^{-1} below the CO–COH deformation mode (≈980 cm^{-1}) and there is no analogous Fermi resonance involving these two modes.

A number of overtone and combination bands can be seen in the mid-IR region. The first overtone of the νC=O vibration (2νC=O) of *cis*-HCOOH, predicted by the anharmonic calculations at 3570.9 cm^{-1}, was detected at 3595.4 cm^{-1}. Both conformers of HCOOH exhibit a weak combination band appearing at slightly lower energies from the CH stretching fundamental. The observed band of the *trans* conformer (ca. 2865.6 cm^{-1}) is assigned to the νC=O + COH–CO def. combination in agreement with [14]. On the other hand, the observed band for *cis* (ca. 2753.4 cm^{-1}) is tentatively assigned to the νC=O + 2τCOH combination mode. The first overtone of the γCH mode of the *cis* conformer could also be expected to give rise to a band in this region, but the assignment of the 2753.4 cm^{-1} band to this vibration can be ruled out because this band is more intense than the γCH fundamental. On the other hand, for *cis*-HCOOH the νC=O is the most intense band and the 2τCOH is one order of magnitude higher in intensity than the γCH fundamental.

The band observed for *trans*-HCOOH at 2397.1 cm^{-1} is assigned to the νC=O + τCOH combination mode. In the gas phase spectrum, two bands were detected in a 50 cm^{-1} interval region centered at this value [14]; the bands were assigned to the first overtone of the CO–COH def. mode (≈2400 cm^{-1}) and the combination of the carbonyl stretching with the O=C–O bending (νC=O + δOCO ≈ 2376 cm^{-1}). In [14], the assignment of the CO–COH def. overtone was made without taking into account the shift induced by the involvement of the fundamental in the Fermi resonance interaction mentioned above. For the unperturbed vibrational level we can expect this overtone to occur well above 2400 cm^{-1}. Therefore, we reject the assignment of the 2397.1 cm^{-1} band to the CO–COH def. overtone. Next, we consider the possible assignment of this band to the νC=O + δOCO mode. It can be approximated that the gas-to-matrix shift of the combination mode roughly follows the arithmetic sum of the gas-to-matrix shift of the two fundamentals involved ($\Delta\nu C{=}O = -9.6$ and $\Delta\delta OCO = +3.3\,cm^{-1}$). Then the νC=O + δOCO combination is expected to lie in the matrix spectrum at ca. 20 cm^{-1} below the observed frequency. The νC=O+ τCOH combination mode is expected to lie at higher wavenumbers than the νC=O + δOCO mode and therefore closer to the observed value in the matrix

Table 1
Observed vibrational frequencies (cm^{-1}) in the mid-IR for the two predominant sites of *trans*- and *cis*-HCOOH/DCOOH isolated in Ar at 8 K and calculated anharmonic vibrational frequencies (CC-VSCF) for the corresponding molecules in the gas phase

Assignment[a]	*trans* Observed		Calculated	*cis* Observed		Calculated
	Site 1	Site 2		Site 1	Site 2	
HCOOH						
	3553.7[w]	3556.7[vw]		3617.2[m]	3615.9[m]	3635.2
νOH	3548.2[m]	3550.5[m]	3551.6			
	3546.7[w]					
2νC═O	3519.0[w]	3515.7[w]	3596.4		3595.4[w]	3570.9
νCH	2956.1[m]	2953.1[m]	2951.4	2899.5[w]	2896.3[w]	2863.1
νC═O + COH–CO def.		2865.6[vw]	2832.7			2875.5
νC═O + 2τCOH				(2759.9[w])	(2753.4[w])	
νC═O + τCOH	(2397.9[vw])	(2397.1[vw])	2348.1			2329.9
CO–COH def. + COH–CO def.			2332.3	2340.1[vw]	2342.3[vw]	2305.5
2COH–CO def.	2196.1[w]	2195.1[w]	2117.1	2206.8[vw]	2198.5[vw]	2136.6
CO–COH def. + δOCO[b]	(1844.1[vw])	(1844.1[vw])				
νC═O	1768.9[vs]	1767.2[vs]	1757.2	1808.0[vs]	1806.9[vs]	1794.9
	1768.3[sh]			1807.8[w]		
	1768.0[m]					
	1764.9[br]					
γCH	1384.4[w]	1381.0[w]	1388.7		1391.8[vw]	1404.2
CO–COH def.	[c]1305.7[w]	[c]1305.7[w]				
	[c]1214.8[w]	[c]1215.8[w]	1267.8	1243.4[s]	1248.9[vs]	1204.3
COH–CO def.	1106.8[vw]	1106.9[vw]	1077.5	1107.3[m]	1104.6[m]	1077.6
	1103.9[s]	1103.6[sh]				
	1100.9[br]	1103.2[s]				
	1094.7[vw]					
ωCH	1037.4[w]	1038.5[w]	1034.6			1014.0
2τCOH			1109.8	979.5[w]	982.6[w]	845.1
	638.6[vw]					
τCOH	635.4[s]	635.4[s]	598.4	502.9[m]	505.3[m]	430.8
δOCO	628.0[m]	629.3[m]	621.0	662.3[w]	662.3[w]	647.3
DCOOH						
	3562.5[vw]	3560.9[vw]				
νOH	3549.9[m]	3551.7[m]	3549.6	3617.4[w]	3615.4[m]	3637.8
	3547.2[vw]			3616.0[m]		
2νC═O	3461.3[vw]	3463.5[vw]				
νCD	2225.2[m]	2225.2[m]	2230.8		2183.5[m]	2167.3
					2179.7[sh]	
νC═O		[d]1761.7[s]	1726.8		[d]1778.7[s]	1761.1
		[d]1761.0[s]			[d]1778.4[m]	
		[d]1759.5[vs]			[d]1777.2[vs]	
		[d]1759.8[sh]				
		[d]1758.1[s]				
					[d]1721.5[m]	
		[d]1723.7[m]			[d]1720.9[m]	
		[d]1722.9[vs]				
ωCD + τCOH				(1370.2[w])	(1372.5[w])	
δCOH	1199.6[w]	1200.3[w]	1255.6	1248.9[vw]	1239.4[vs]	1193.9
				1234.0[vs]		
				1229.1[vw]		
νC–O	1142.1[s]	1141.7[s]	1126.7	1143.4[m]		1125.4
	1144.4[w]					
2τCOH				996.3[w]	995.1[w]	840.5
γCD	976.2[s]	974.1[s]	981.2	961.9[w]	962.9[w]	985.7
	974.9[w]					
ωCD	874.8[w]	875.0[w]	875.8			866.2
	667.7[vw]	667.7[vw]				
	629.8[w]					
τCOH	626.4[m]	625.9[m]	589.4		500.7[w]	425.4
					498.1[w]	
δOCO	622.3[m]	623.5[m]	615.2	655.2[vw]	655.2[vw]	640.8

Qualitative information on intensities is given as superscript: vs, very strong; s, strong; m, medium; w, weak; vw, very weak; sh, shoulder; br, broad.

[a] According to [11]: ν, stretching; δ, bending; γ, rocking; ω, wagging, def., deformation.

[b] According to [14].

[c] Components of a Fermi resonance doublet between the first overtone of τCOH and the CO–COH def. observed only for *trans*-HCOOH.

[d] Components of a Fermi resonance doublet between the first overtone of the ωCD and νC═O modes.

Frequency values centered between site 1 and site 2 columns could not be assigned to a specific site due to lack of site selective data. Values in parentheses are tentatively assigned. An explanation about the assignment of several bands to the same mode in the site-selective spectra is given in the text.

Table 2
Observed vibrational frequencies (cm^{-1}) in the near-IR for the two predominant sites of *trans*- and *cis*-HCOOH isolated in Ar at 8 K and calculated anharmonic vibrational frequencies (CC-VSCF) for the corresponding molecules in gas phase

Assignment	*trans*-HCOOH		Gas phase[a]	Calc.	*cis*-HCOOH		Calc.
	Ar site 1	Ar site 2			Ar site 1	Ar site 2	
2νOH	6930.3^{s}	6934.8^{s}	6968	6943.7	7062.3^{s}	7065.7^{m}	7053.8
2νCH + ωCH			6773				
νOH + νCH			6507	6431.0			6425.6
νCH + 2νC═O	6411.2^{vw}		6440				
	6407.0^{vw}						
2νCH	5803.0^{vw}		5775	5788.3			5604.0
	5797.3^{vw}						
νCH + 2γCH			5592				
νOH + νC═O	5316.4^{m}	5317.2^{m}	5343	5236.2			5347.2
νOH + γCH	4928.7^{m}	4926.1^{w}	4942	4863.5			4960.1
		4841.2^{sh}					
νOH + 2τCOH[b]	(4838.7^{m})	(4839.8^{m})	4857				
νOH + CO–COH def.[b]	(4757.2^{m})	(4759.4^{m})	4780	4686.1	4847.7^{m}	4854.4^{s}	4704.8
2νC═O + CO–COH def.		(4752.2^{br})					
?	4712.0						
νCH + νC═O	4707.0^{vw}	4706.0^{m}	4708	4708.3	4704.0^{w}	4700.0^{m}	4666.2
νOH + COH–CO def.	4649.6^{m}	4651.4^{m}	4670	4534.7	4716.2^{m}	4712.5^{w}	4622.6
νOH + ωCH			4600	4517.6			4576.6
2γCH + νC═O	4510.0^{vw}		4515			4553.4^{vw}	
νCH + γCH	4317.0^{w}		4300	4287.4			4219.3
νC═O + 2CO–COH def.	(4270.4^{w})						
νCH + 2τCOH[b]	(4254.2^{w})	(4252.0^{w})	4242				
νOH + τCOH	(4183.6^{m})	(4185.2^{m})	4209	4102.2	(4110.0^{vw})	(4111.5^{vw})	4130.2
νCH + CO–COH def.[b]	(4171.8^{w})	(4175.1^{w})		4214.4			4098.7
νOH + δOCO	(4167.4^{vw})		4192	4085.8	4277.3^{vw}	4275.9^{vw}	4195.8
?	4157.7^{vw}						
νCH + COH–CO def.	4059.7^{w}	4055.3^{w}	4043	4026.6			

Qualitative information on intensities is given as superscript: vs- very strong; s, strong; m- medium; w, weak; vw, very weak; sh, shoulder; br, broad. Frequencies in parentheses correspond to tentative assignments.

[a] From [14]. ν, stretching; δ, bending; γ, rocking; ω, waging; def., deformation.

[b] Ascribed as components of a Fermi resonance doublet between the combination modes νOH(νCH) + 2τCOH and νOH(νCH) + CO–COH def. of the *trans* conformer.

making this assignment most plausible. No bands were observed in the matrix spectrum that could be ascribed to the 2CO–COH def. or νC═O + δOCO modes.

The CO–COH def. + COH–CO def. combination band was observed for *cis*-HCOOH at 2342.3 cm^{-1} and calculated at 2305.5 cm^{-1}. The corresponding mode was not detected for the *trans* conformer, in agreement with its predicted lower intensity (four times lower than in the *cis* conformer). The very weak band observed for *cis*-HCOOH at 2198.5 cm^{-1} is ascribed to the overtone of the COH–CO def. mode, which in the *trans* conformer gives rise to the band at 2195.1 cm^{-1} [11].

Following the gas phase assignment [14], the very weak band observed for *trans*-HCOOH at 1844.1 cm^{-1} is tentatively ascribed to the CO–COH def. + δOCO combination. However, its assignment to the CO–COH def. + τCOH mode is also possible. Indeed, for *trans*-HCOOH it is difficult to distinguish the combination modes involving δOCO or τCOH because these two fundamentals appear at similar frequencies. Note that in the case of the *cis* conformer the τCOH and δOCO fundamentals are separated by approximately 155 cm^{-1}, which allows us to reliably distinguish the combination modes involving each vibration.

For DCOOH the C═O stretching mode participates in a very strong Fermi resonance with the first overtone of the CD wagging mode (2ωCD) in both isomers (see Table 1) [10,11]. Therefore, the previously discussed dependency of the νC═O on the conformation is not observed for DCOOH, with both conformers giving rise to bands at similar frequency values. The 2ωCD is predicted to be more than two orders of magnitude lower in intensity than the νC═O for both conformers of DCOOH. However, the observed ratio of intensities (2ωCD : νC═O) is roughly 1:2 and 1:5 for *trans*- and *cis*-DCOOH, respectively, due to the involvement of the two vibrations in the Fermi resonance interaction. Despite the larger intensity ratio of the Fermi doublet for *trans*-DCOOH, the observed frequency splitting between the components is larger for *cis*-DCOOH (ca. 57 and 37 cm^{-1} in *trans*-DCOOH). Accordingly, the Fermi resonance coupling coefficients (W), obtained from a standard perturbative analysis [32], for *cis*- and *trans*-DCOOH are ca. 21 and 18 cm^{-1}, respectively, also

Table 3
Observed near-IR active vibrational frequencies (cm^{-1}) of the *trans* conformer of DCOOH, HCOOD and DCOOD isolated in Ar at 8 K[a] and calculated anharmonic vibrational frequencies (CC-VSCF) for the corresponding molecules in gas phase

DCOOH				HCOOD				DCOOD			
Assignment	Ar	Gas phase[b]	Calc.	Assignment	Ar	Gas phase[b]	Calc.	Assignment	Ar	Gas phase[b]	Calc.
2νOH	6937.4	6975	6939.4	2νOD	5152.9	5181	5163.6	2νOD	5152.9	5181	5169.1
	6933.3				5149.7				5149.7		
νOH + νCD	5773.2		5708.9	νOH + νCD			5547.2	νOD + νCD			4823.5
2νCD	4401.2	≈4360[e]	4400.8	2νCH			5791.3	2νCD			4398.7
νOH + 2ωCD[c]	(5312.0)			νOD + νC=O	4382.2	4404	4345.8	νOD + νC=O			4318.3
νOH + νC=O[c]	(5273.9)		5205.5		4380.0						
νOH + 2τCOH[d]	(4835.1)	4850									
	(4825.3)										
νOH + δCOH[d]	(4743.3)	4781	4649.5								
	(4740.9)										
νOH + γCD			4451.5								
νOH + ωCD			4356.5								
				νCH + γCH	.		4275.8				
νCD + 2ωCD[c]	(3974.3)	3980		νCH + νC=O	4723.7	4736	4704.3	νCD + νC=O	3987.1	3981	3949.2
νCD + νC=O[c]	(3937.3)		3953.4		4721.1	4702					
νOH + νCO	4693.2	4701	4593.1	νCH + νCO	4142.6	4144	4114.4				
	4691.7				4141.2	4115					
νOH + τCOH	4175.4		4098.6	νCH + ωCH	3990.2		3926.9				
	4173.3				3988.2						
νOH + δOCO	4170.2	4201	4076.2								
	4166.7			νCH + 2τCOD	3946.2						
				νCH + δCOD	.		3923.4				

[a] The majority of the modes appear site-splitted.
[b] From [13].
[c] Components of a Fermi resonance doublet between the combination modes νOH(νCD) + 2ωCD and νOH(νCD) + νC=O.
[d] Fermi resonance doublet between the combination modes νOH + 2τCOH and νOH + δCOH.
[e] Band center of the observed doublet ascribed to rotational structure. ν, stretching; δ, bending; γ, rocking; ω, wagging; def., deformation. Frequencies in parentheses correspond to tentative assignments.

pointing to a stronger coupling between the νC=O and the 2ωCD in the *cis* form.

It has been suggested that the COH bending (δCOH) in *trans*-DCOOH is also involved in a Fermi interaction together with the 2τCOH mode (the τCOH fundamental appears at ≈626 cm^{-1}) [11]. This is supported by our observation that the δCOH absorption band in *cis*-DCOOH is much higher in energy (1239.4 cm^{-1}) than the corresponding band for *trans*-DCOOH (1200.3 cm^{-1}), although the calculations predict the opposite trend (see Table 1). The Fermi resonance in *trans*-DCOOH shifts the δCOH level down. In *cis*-DCOOH the overtone of the τCOH mode is observed at 995.1 cm^{-1}, which is too low to enable its involvement in a Fermi resonance with the δCOH mode.

The τCOH fundamental mode is observed at ≈500 cm^{-1} for the *cis* conformer in both HCOOH and DCOOH. This vibration is shifted ≈130 cm^{-1} towards lower wavenumbers when compared with the same vibration in the *trans* conformer (see Table 1). The repulsive interaction between the C=O and O–H bond dipoles resulting from their nearly parallel alignment and the steric repulsion between the hydrogen atoms lying on the same side of the C–O bond in the *cis* configuration have been pointed out as the major factors responsible for the higher energy of the *cis* conformer when compared with the *trans* form [18]. Indeed, these effects partially destabilize the *cis* planar conformations of this molecule with respect to the non-planar conformations. Thus, it leads to a softer torsional energy profile around this conformer and decreases the force constant of the torsion.

6. Near-IR region

In this section, we analyze the near-IR (7900–4000 cm^{-1}) spectra of the two conformers of formic acid, the discussion being focused on site 2. The OH stretching absorption bands of *trans*-formic acid were used to promote the site-selective rotamerization process (Fig. 3). Table 2 presents the observed vibrational frequencies for both HCOOH conformers and the results of the anharmonic vibrational calculations. Table 3 collects the observed and calculated vibrational frequencies for *trans*-DCOOH, HCOOD, and DCOOD omitting site labeling.

The first OH stretching overtone of *trans*-HCOOH is observed at 6934.8 cm^{-1} and predicted by the calculations at 6943.7 cm^{-1}, both of them being in good

agreement with the existing gas phase data (6968 cm^{-1} [14]). For *cis*-HCOOH the same mode is predicted by the calculations at 7053.8 cm^{-1} and observed at 7065.7 cm^{-1}. The experimentally determined anharmonicity constant for the OH stretching mode of *cis*-HCOOH is ca. $-85\,cm^{-1}$, which is very close to the values obtained for the *trans* conformer (ca. $-83\,cm^{-1}$ and $-91 cm^{-1}$, matrix isolated and gas phase [14], respectively). The $\nu OH + \nu CH$ mode, observed in the gas phase for *trans*-HCOOH at 6507 cm^{-1}, was not found in our matrix studies. For *trans*-DCOOH a band appearing at 5773.2 cm^{-1} is assigned to the $\nu OH + \nu CD$ mode (predicted by the CC-VSCF calculations at 5708.9 cm^{-1}).

For *trans*-HCOOH, the medium intensity bands observed at 4839.8 and 4759.4 cm^{-1} are here ascribed to the $\nu OH + 2\tau COH$ and $\nu OH +$ CO–COH def. combination modes. Considering the observed fundamental vibrations, it is reasonable to assign the higher frequency band to a combination mode involving the νOH fundamental and the overtone of δOCO or τCOH. In both cases, the observed combination mode would be shifted up from the expected value (even without taking into account the anharmonicity). This could be explained by a Fermi resonance coupling with a mode laying at similar wavenumbers. As discussed earlier, in the mid-IR region the 2τCOH and CO–COH def. modes are coupled by Fermi resonance, and it is plausible that the combination mode of each of these vibrations with the same νOH fundamental is also perturbed in a similar way. In the gas phase [14], the band at 4857 cm^{-1} was tentatively assigned to the $\nu OH + 2\tau COH$ combination mode while the band at 4780 cm^{-1} was assigned to the $\nu OH +$ CO–COH def. combination mode. In [14], the existence of the Fermi resonance coupling between the 2τCOH and CO–COH def. modes was ignored, and the perturbed vibrational levels were used to estimate the position of the combination modes. In *cis*-HCOOH, only one band that can be ascribed to the $\nu OH +$ CO–COH def. is observed in the 4900–4700 cm^{-1} region (4854.4 cm^{-1}). This is in agreement with the fact that the $\nu OH + 2\tau COH$ combination mode is expected to occur at significantly lower wavenumbers (in the 4600–4500 cm^{-1} region, see Table 1), therefore preventing its involvement in a Fermi resonance of the same type as that observed for *trans*-HCOOH.

The *cis*-HCOOH absorption band at 4700.0 cm^{-1} is ascribed to the $\nu CH + \nu C{=}O$ combination, observed for *trans*-HCOOH at 4706.0 cm^{-1} (see site 2 data in Table 2). The *cis*-band at 4712.5 cm^{-1} is assigned to the $\nu OH +$ COH–CO def. combination, observed at a frequency ca. 60 cm^{-1} higher than that of the *trans*-conformer (4651.4 cm^{-1}). The magnitudes of the coupling constants for these two modes seem to be reversed in *cis*-HCOOH (coupling constant $x_{ij} = \nu_{i+j} - \nu_i - \nu_j \approx -3.2$ and $-8.0\,cm^{-1}$ for $\nu CH + \nu C{=}O$ and $\nu OH +$ COH–CO def., respectively) when compared to *trans*-HCOOH ($x_{ij} \approx -14.3\,cm^{-1}$ and $-2.3\,cm^{-1}$, respectively). However, the alternative assignment of the lower frequency band to the $\nu CH + \nu C{=}O$ would result in a positive coupling constant for the $\nu CH + \nu C{=}O$ mode, which seems unlikely.

In the 4200–4150 cm^{-1} region few bands are observed for both isomers that are tentatively assigned. Three site-splitted bands are observed for *trans*-HCOOH, ascribed to the $\nu OH + \tau COH$, $\nu OH + \delta OCO$, and $\nu CH +$ CO–COH def. combination modes (see Table 2). The assignment of these bands follows that made previously in [14]. A very weak band observed at 4111.5 cm^{-1} for *cis*-HCOOH can be due either to the $\nu OH + \tau COH$ combination mode (the sum of the fundamentals gives ca. 4120 cm^{-1}) or the $\nu CH +$ CO–COH def. vibration (the sum of the fundamentals gives ca. 4144 cm^{-1}). The $\nu OH + \delta OCO$ combination band is observed for *cis*-HCOOH at ca. 4276 cm^{-1} as a weakly coupled mode (the sum of the fundamentals is ca. 4278 cm^{-1}). As already mentioned, the difference between the observed frequencies for the τCOH and δOCO fundamentals in *cis*-HCOOH allows us to reliably separate the combination modes involving each one of these vibrations.

For *trans*-DCOOH the bands observed at ≈4830 and 4740 cm^{-1} are tentatively assigned to a Fermi resonance doublet involving $\nu OH + 2\tau COH$ and $\nu OH + \delta COH$, in a similar way to what was found for *trans*-HCOOH. Another Fermi resonance doublet was observed in the *trans*-DCOOH spectrum coupling the $\nu OH + 2\omega CD$ with the $\nu OH + \nu C{=}O$ (see Table 3). The splitting between this Fermi resonance doublet is identical to that observed in the mid-IR for the very strong Fermi resonance doublet involving the 2ωCD and νC=O modes (ca. 37 cm^{-1}). The unperturbed frequencies of the 2ωCD and νC=O vibrations are estimated to be ca. 1746 and 1738 cm^{-1}, respectively. The unperturbed $\nu OH + 2\omega CD$ and $\nu OH + \nu C{=}O$ combination modes are expected at ca. 5297 and 5289 cm^{-1}, respectively, using site averaged values and without taking into account the intermode coupling constant. By comparison of these values with the observed combination bands (5312 and 5274 cm^{-1}), we estimate a Fermi resonance induced shift relative to the unperturbed positions of 15 cm^{-1}, exactly the same as that calculated for the mid-IR active Fermi doublet due to $\nu C{=}O$ and $2\omega CD$.

In Table 4, we present several observed and calculated (CC-VSCF) coupling and anharmonicity constants for *cis*- and *trans*-HCOOH together with the corresponding gas phase data [14]. By comparing the coupling constants obtained for *trans*-HCOOH isolated in argon with the gas phase data, we conclude that the cage potential affects significantly the guest intermode couplings. These changes in the coupling constants are in many cases of similar magnitude as the constants

Table 4
Observed and CC-VSCF calculated anharmonicities and coupling constants[a] for *cis*- and *trans*-HCOOH

	trans-HCOOH				*cis*-HCOOH		
	Site 1	Site 2	Gas phase[b]	Calc.	Site 1	Site 2	Calc.
Combinations	Coupling constants (x_{ij}, cm^{-1})						
νOH + νC=O	−0.7	−0.5	−1.2	−72.6			−82.9
νOH + γCH	−3.9	−5.4	−3.6	−76.8			−79.3
νOH + CO–COH def.				−133.3	−12.9	−10.4	−134.7
νOH + COH–CO def.	−2.5	−2.3	−1.8	−94.4	−8.3	−8.0	−90.2
νOH + ωCH			−1.0				
νOH + τCOH	(0)	(−0.7)	(−2.2)	−47.8	(−10.1)	(−9.7)	+64.2
νOH + δOCO	(−15.5)		(−4.7)	−86.8	−2.2	−2.3	−86.7
νCH + νC=O	−18.0	−14.3	−5.4	−0.3	−3.5	−3.2	−8.2
νCH + γCH	−23.5	−17.1	−22.1	−52.7			−48.0
νCH + COH–CO def.	−0.3	−1.0	−1.8	−2.3			−7.7
νCH + ωCH			−5.7				
νC=O + COH–CO def.		−4.8	−2.6	−2.0			−3.0
νC=O + τCOH	(−6.4)	(−5.5)		−7.5			−104.2
CO–COH def. + COH–CO def.				−7.0	−10.6	−11.2	−23.6
Overtones	Anharmonicity constants (x_{ij}, cm^{-1})						
2νOH	−83.1	−83.1	−91.2	−79.8	−86.1	−83.1	−108.3
2νCH	−53.1		−52.4	−57.3			−61.1
2νC=O	−9.4	−9.4	−9.3	−9.0		−9.2	−9.5
2COH–CO def.	−5.9	−5.7	−6.6	−19.0	−3.9	−5.4	−9.3
2τCOH				−43.5	−13.2	−14.0	−8.3

[a] $x_{ij} = \nu_{i+j} - \nu_i - \nu_j$; $x_{ii} = (2\nu_i - 2.\nu_i)/2$.
[b] Gas phase data was taken from [14].
Values in parentheses were calculated based on a tentative assignment. Values centered between site 1 and site 2 columns are average estimates for the two sites.

themselves. Moreover, changing of the matrix trapping site leads also to significant effects on the anharmonicity and intermode couplings (see, for example, the constants of either νCH + νC=O or νCH + γCH modes in Table 4). It can then be concluded that the local environment is an important factor to be considered in the processes involving intramolecular vibrational redistribution and relaxation in solid phase. The average difference between the constants estimated for both sites and the gas phase values is approximately the same in both conformers, which means that the local environment perturbs both conformers to a similar extent.

7. Anharmonic calculations

The equilibrium structures and harmonic vibrational properties of the conformers of formic acid are rather well reproduced at the MP2/6-311++G(2d,2p) level of theory employed previously in our studies of HCOOH [27,28]. The harmonic and anharmonic vibrational frequencies computed for *trans*- and *cis*-HCOOH are compared in Table 5. The anharmonic effects are most significant for the high-frequency modes, i.e. the OH and CH stretches, for which the anharmonic calculations reduce the obtained frequencies by $\approx 200\,cm^{-1}$ from the harmonic values. The CC-VSCF calculations give a good reproduction of the experimentally observed positions for most of the fundamental frequencies. Only the skeletal deformation modes (CO–COH def. and COH–CO def.) and the torsional mode seem to be troublesome. For example, the CC-VSCF calculations predict the torsional mode to be *ca.* 40 and $70\,cm^{-1}$ below the experimental values of *trans*- and *cis*-HCOOH, respectively (see Table 5). The infrared intensities obtained both in the harmonic and anharmonic calculations are rather similar and both follow qualitatively the experimentally observed data.

The CC-VSCF calculations reveal a rather rich overtone and combination band spectrum for both conformers in qualitative accord with the experimentally observed spectra. However, the numerical agreement between the experimentally found vibrational frequencies and the CC-VSCF ones are not as good as in the case of the fundamental modes. For the first overtones of the OH and CH stretching modes, the calculations give reasonable estimates of the band positions. On the other hand, most of the combination bands and overtones involving one or several skeletal deformation modes seem to be a challenge for the CC-VSCF method. The results of the anharmonic CC-VSCF calculations are compared with the experimental data in Table 4 in the form of computed anharmonicity and coupling constants for the observed overtone and combination bands. The errors made in computing the fundamentals are reflected in the overtones and combination modes,

Table 5
Harmonic and anharmonic vibrational frequencies (cm^{-1}) and infrared intensities (in parentheses) of *trans*- and *cis*-formic acid[a]

	trans-HCOOH						*cis*-HCOOH					
	ν_{harm}		ν_{anh}		ν_{exp}^{Ar}		ν_{harm}		ν_{anh}		ν_{exp}^{Ar}	
2νOH			6943.7	(4)	6933	(13)			7053.8	(3)	7064	(10)
2νCH			5788.3	(1)	5800	(< 1)			5604.0	(1)		
νOH + νC=O			5236.2	(3)	5317	(2)						
νOH + γCH			4863.5	(1)	4927	(2)						
νOH + CO–COH def.					4758[b]	(2)			4704.8	(37)	4851	(2)
νCH + νC=O			4708.3	(4)	4707	(1)			4666.2	(5)	4702	(2)
νOH + COH–CO def.			4534.7	(11)	4651	(2)			4622.6	(2)	4714	(< 1)
νCH + CO–COH def.			4214.4	(2)	4173[b]	(1)			4098.7	(1)		
νOH + τCOH			4102.2	(83)	4184	(5)			4130.2	(39)	4111	(7)
νCH + COH–CO def.			4026.6	(1)	4058	(1)						
νOH	3784.0	(171)	3551.6	(217)	3549	(320)	3851.5	(171)	3635.2	(221)	3617	(380)
2νC=O			3496.4	(9)	3517	(14)			3570.9	(8)	3595	(15)
3CO-COH def.									3520.8	(11)		
νC=O + γCH			3140.2	(1)								
3COH–CO def.			3108.8	(1)								
νCH	3134.2	(69)	2951.4	(71)	2955	(80)	3046.1	(134)	2863.1	(118)	2898	(120)
νC=O + COH–CO def.			2832.7	(12)	2866	(6)			2875.5	(6)		
2γCH			2774.4	(1)					2806.4	(2)		
CO–COH def. + COH–CO def.			2338.3	(3)					2305.5	(12)	2341	(17)
2COH–CO def.			2117.1	(13)	2196	(16)			2136.6	(2)	2203	(6)
2ωCH			2077.7	(4)					2035.7	(3)		
νC=O	1788.8	(696)	1757.2	(997)	1768	(1000)	1829.2	(558)	1794.9	(826)	1807	(850)
COH–CO def. + δOCO			1697.8	(2)								
3τCOH			1616.9	(68)					1457.8	(41)		
COH–CO def. + τOCO			1594.6	(2)								
γCH	1426.5	(3)	1388.7	(13)	1383	(19)	1441.7	(< 1)	1404.2	(7)	1392	(2)
CO–COH def.	1316.6	(20)	1267.8	(34)	1215[b]	(53)	1287.2	(615)	1204.3	(749)	1246	(933)
2τCOH			1109.8	(34)	1306[b]	(17)			845.1	(1)	981	(16)
COH–CO def.	1123.3	(586)	1077.5	(618)	1103	(757)	1113.0	(164)	1077.6	(170)	1106	(250)
ωCH	1065.3	(8)	1034.6	(1)	1038	(11)	1042.9	(< 1)	1014.0	(2)		
τCOH	676.8	(298)	598.4	(320)	635	(500)	536.8	(184)	430.8	(156)	504	(240)
δOCO	631.7	(82)	621.0	(109)	629	(171)	661.2	(24)	647.3	(26)	662	(16)

[a] Calculated infrared intensities (in km/mol) and experimental integrated intensities were normalized so that the most intense band of the *trans* conformer has an intensity of 1000. After this procedure all the predicted combination and overtone bands with intensities less than 1 are omitted. Experimental band positions correspond to the average value of the observed bands for the molecules isolated in two matrix-sites. The intensities of the anharmonic vibrations were obtained from Hartree–Fock wave functions in the CC-VSCF calculations.

[b] Bands involved in Fermi resonance coupling. These bands should not be compared with the calculated values.

and thus in many cases the coupling constants are overestimated. There can be several reasons for the discrepancy of the observed and computed vibrational frequencies. The CC-VSCF calculations involve an approximation of separability of normal coordinates used to describe the vibrational motions of the molecule [23–25]. Therefore, if strong couplings exist between modes the CC-VSCF calculations are not able to reproduce these motions. Also, the wide-amplitude vibrational modes, like the torsion in formic acid, seem to be hard to describe sufficiently well. Additionally, it must be remembered that the computational level used here (MP2/6-311++G(2d,2p)) could prove less reliable for configurations further away from the equilibrium structure. All in all, the CC-VSCF method is able to reproduce the experimental characteristics of formic acid on a qualitative level and it is more suitable to support experimental identification of molecular species than the standard harmonic vibrational calculations.

8. Conclusions

Vibrational spectroscopic data on matrix-isolated *cis*- and *trans*-HCOOH and DCOOH in different sites is presented. The 7900–4000 cm^{-1} spectral features for *cis*-HCOOH are discussed for the first time. This study also presents for the first time the experimental vibrational spectra of *cis*-DCOOH.

For *trans*-HCOOH all but two of the CC-VSCF predicted binary combinations and first overtones in the 7000–4000 cm^{-1} region were detected. For *cis*-HCOOH about half of the expected modes were observed, in spite of the presence of this conformer in the matrix in a lower

concentration. A very strong Fermi resonance between νC=O and 2ωCD, previously reported for *trans*-DCOOH, was also found to be present in the *cis* conformer. The observed combinations of these two modes with the νOH were also found to be involved in Fermi resonance.

From the site-selective data, we conclude that the cage potential affects significantly the guest intermode coupling. The effect of local morphology on the anharmonicity and intermode couplings was found to be comparable with the effect of going from the gas phase to the solid rare gas environment. Therefore, we expect an important contribution from the local environment to the dynamics of processes involving intramolecular vibrational redistribution and relaxation in solid phase.

The CC-VSCF calculations reproduce reasonably well the experimentally observed positions of the fundamental frequencies, excluding the skeletal deformation modes and the torsional vibration. The coupling constants are overestimated by the calculations. The absolute shifts from the experimental values for the combination bands and overtones are twice as high as the ones for fundamentals, nevertheless, the relative error is still small (≈3%). The systematic underestimation of the vibrational frequencies might be an indication that the ab initio potential energy surface used is too "soft." Despite of that, the CC-VSCF calculations were shown to be superior to the standard harmonic vibrational predictions, and their ability to contribute to the assignment of overtone and combination modes appears as a valuable tool to aid the experimental work.

Acknowledgments

The Academy of Finland and Finnish Cultural Foundation are thanked for financial support. E.M. and R.F. acknowledge the Portuguese Foundation for Science and Technology (Ph.D. grant SFRH/BD/4863/2001 and project POCTI7433667QUI/2001). Prof. Benny Gerber and Dr. Galina Chaban are thanked for discussions on the anharmonic vibrational calculations

References

[1] S.-Y. Liu, D.M. Mehringer, L.E. Snyder, J. Astrophys. 552 (2001) 654–663.
[2] A. Goldman, F.H. Murcray, D.G. Murcray, C.P. Rinsland, Geophys. Res. Lett. 11 (1984) 307–310.
[3] B. Elves, S. Hawkins, M. Ravenscroft, J.F. Rounsaville, G. Schulz (Eds.), Ullmann's Encyclopedia of Industrial Chemistry, vol. A12, fifth ed., VCH, Germany, 1989.
[4] R.C. Millikan, K.S. Pitzer, J. Chem. Phys. 27 (1957) 1305–1308.
[5] I.C. Hisatsune, J. Heicklen, Can. J. Spectrosc. 18 (1973) 135–142.
[6] G.M.R.S. Luiz, A. Scalabrin, D. Pereira, Infrared Phys. Technol. 38 (1997) 45–49.
[7] T.L. Tan, K.L. Goh, P.P. Ong, H.H. Teo, J. Mol. Spectrosc. 198 (1999) 110–114, and references therein.
[8] J.E. Bertie, K.H. Michaelian, J. Chem. Phys. 76 (1982) 886–894.
[9] T. Miyazawa, K.S. Pitzer, J. Chem. Phys. 30 (1959) 1076–1086.
[10] R.L. Redington, J. Mol. Spectrosc. 65 (1977) 171–189.
[11] D.O. Henderson, Doctoral Thesis, Texas Technical University, 1987.
[12] F. Madeja, P. Markwick, M. Havenith, K. Nauta, R.E. Miller, J. Chem. Phys. 116 (2002) 2870–2878.
[13] H. Morita, S. Nagakura, J. Mol. Spectrosc. 41 (1972) 54–68.
[14] M. Freytes, D. Hurtmans, S. Kassi, J. Liévin, J. Vander Auwera, A. Campargue, M. Herman, Chem. Phys. 283 (2002) 47–61.
[15] W.M. Hocking, Z. Naturforsch 31A (1976) 1113–1121.
[16] P.G. Blake, H.H. Davies, G.E. Jackson, J. Chem. Soc. B (1971) 1923.
[17] M. Pettersson, J. Lundell, L. Khriachtchev, M. Räsänen, J. Am. Chem. Soc. 119 (1997) 11715–11716.
[18] K.B. Wiberg, K.E. Laidig, J. Am. Chem. Soc. 109 (1987) 5935–5943.
[19] J.D. Goddard, Y. Yamaguchi, H.F. Schaefer III, J. Chem. Phys. 96 (1992) 1158–1166.
[20] M. Pettersson, E.M.S. Maçôas, L. Khriachtchev, J. Lundell, R. Fausto, M. Räsänen, J. Chem. Phys. 117 (2002) 9095–9098.
[21] S. Sander, H. Willner, L. Khriachtchev, M. Pettersson, M. Räsänen, E.L. Varetti, J. Mol. Spectrosc. 203 (2000) 145–150.
[22] L. Khriachtchev, J. Lundell, E. Isoniemi, M. Räsänen, J. Chem. Phys. 113 (2000) 4265–4273.
[23] J.O. Jung, R.B. Gerber, J. Chem. Phys. 105 (1996) 10332–10348.
[24] J.O. Jung, R.B. Gerber, J. Chem. Phys. 105 (1996) 10682–10690.
[25] G.M. Chaban, J.O. Jung, R.B. Gerber, J. Chem. Phys. 111 (1999) 1823–1829.
[26] G.M. Chaban, J.O. Jung, R.B. Gerber, J. Phys. Chem. A 104 (2000) 2772–2779.
[27] J. Lundell, M. Räsänen, Z. Latajka, Chem. Phys. 189 (1994) 245–260.
[28] J. Lundell, Chem. Phys. Lett. 266 (1997) 1–6.
[29] M.W. Schmidt, K.K. Baldridge, J.A. Boatz, S.T. Elbert, M.S. Gordon, J.H. Jensen, S. Koseki, N. Matsunaga, K.A. Nguyen, S.J. Su, T.L. Windus, M. Dupuis, J.A. Montgomery, J. Comput. Chem. 14 (1993) 1347–1363.
[30] E. Bjarnov, W.M. Hocking, Z. Naturforsch. 33A (1978) 610–618.
[31] R. Fausto, A.E. Batista de Carvalho, J.J.C. Teixeira-Dias, M.N. Ramos, J. Chem. Soc. Faraday Trans. 85 (2) (1989) 1945–1962.
[32] G.S. Devendorf, M.-H.A. Hu, D. Ben-Amotz, J. Phys. Chem. A. 102 (1998) 10614–10619.